Beamforming in an annular duct with swirling flow

Sijtsma, P.; Brouwer, Harry; Snellen, M.

DOI
10.2514/6.2023-3840

Publication date
2023

Document Version
Final published version

Published in
AIAA AVIATION 2023 Forum

AIAA AVIATION Forum
12-16 June 2023, San Diego, CA and Online
AIAA AVIATION 2023 Forum

10.2514/6.2023-3840

Beamforming in an annular duct with swirling flow

Pieter Sijtsma*
PSA3, 9493 TE De Punt, The Netherlands

Harry Brouwer†
Netherlands Aerospace Centre NLR, 1059 CM Amsterdam, The Netherlands

Mirjam Snellen‡
Delft University of Technology, 2629 HS Delft, The Netherlands

The fan-stator stage of turbofan engines is one of the main regions of broadband noise generation. The trend of increasing bypass ratios will make fan-stator broadband noise even more significant, as jet noise will decrease and nacelles will become shorter, thus leaving less space for liners. Within the fan-stator stage there are several aerodynamic phenomena that can cause broadband noise. However, techniques for experimental identification and quantification (and thus classification) of these broadband noise sources are still immature. Beamforming using in-duct microphones is feasible, but a major challenge is the strong rotational component of the flow that needs to be accounted for in the steering vectors. This paper proposes a solution for that challenge, based on a fast ray tracing approach. With synthesized microphone array data, calculated with an approximate method for the Green's function in a ducted swirling flow, it is demonstrated that detection of acoustic sources is possible.

Nomenclature

A	source amplitude [Pa.s]	N	number of microphones
a	source signal [Pa]	P_n	microphone amplitude [Pa.s]
c	sound speed [m/s]	p_n	microphone signal [Pa]
c_0	sound speed at tip [m/s]	R	tip radius [m]
f	frequency [Hz]	r	radial coordinate, $r=\sqrt{y^2+z^2}$
He	dimensionless frequency	$\vec{U}$	flow speed [m/s]
h	hub radius [m]	$\vec{v}$	view direction
i	imaginary unit	$\vec{w}$	shoot direction
k	wave number [1/m]	x, y, z	cartesian coordinates [m]
$\vec{k}$	wave-slowness vector [s/m]	$\vec{x}_n$	microphone location
M_x	axial flow Mach number	Z	dimensionless wall impedance
M_θ	rotational flow Mach number	α, β	coefficients in Eq. (5)
$M_{\theta,\text{hub}}$	rotational flow Mach number at hub	Δt	time delay [s]
$M_{\theta,\text{tip}}$	rotational flow Mach number at tip	$\vec{\xi}$	source location

I. Introduction

In the past decades there has been a trend of increasing the fan diameter of aircraft turbofan engines. This has led to reduction of jet speed and thereby to less fuel consumption and less jet noise. The next step is the development of Ultra-High-Bypass Ratio (UHBR) engines. Due to the decreasing significance of jet noise and the reduction of nacelle length, the noise produced in the fan-stator area ("fan noise") is getting increasingly important. To reduce fan noise, detailed knowledge about the mechanisms and the locations of noise generation is necessary.

* Director; also at Aircraft Noise & Climate Effects (ANCE) Section, Faculty of Aerospace Engineering, Delft University of Technology, The Netherlands
† Senior Scientist, Department of Vertical Flight and Aeroacoustics, P.O. Box 90502
‡ Professor, Aircraft Noise & Climate Effects (ANCE) Section, Faculty of Aerospace Engineering, Kluyverweg 1

Beamforming with an array of microphones[1] is the most obvious approach to detect the noise source locations. However, finding those locations in a confined annular region with high-speed swirling flow is quite a challenge, in addition to the challenge of mounting the microphones at the most suitable locations in the area of interest.

For finding noise source locations, high-fidelity numerical predictions[2] can be a good alternative to measurements. Beamforming can be applied to numerical data as well. The advantage of numerical predictions is that "microphones" can be placed anywhere in the computation domain. A disadvantage is the short time duration of computational data, which limits the applicability of advanced methods that assume source incoherence[3-5].

A few attempts of performing "in-duct beamforming" using measured data in a turbofan engine have been reported[6-9]. In some cases, noise sources could be identified, but in general the success was limited due to (hard wall) reverberation and limited spatial resolution.

Reverberation can be compensated for by using in-duct ("tailored") Green's functions for the acoustic transfer model in the beamforming algorithm. For a straight annular duct containing uniform axial flow, Rienstra and Tester[10] derived an analytic expression, featuring a summation of duct modes. Sijtsma[11] developed a method for calculating the Green's function in a sheared axial flow. This was done by dividing the annulus into a number of segments with uniform flow. A general Green's function formulation with radially varying axial and rotational flow was derived by Mathews and Peake[12]. Brouwer and Sijtsma[13] developed a fast implementation, using segments with solid body swirl. All these Green's function formulations can deal with both hard and lined walls.

The use of in-duct Green's functions may seem natural, but it brings in some hazards, especially in the case of hard walls. Side lobe patterns, which can falsely be identified as sources, may appear, particularly at frequencies close to cut-off[13]. Furthermore, Green's functions assume a specific source directivity, like a monopole or a dipole, which can be different from reality. This may lead to an overcorrection for wall reflections. Further obvious disadvantages of in-duct Green's functions are the assumptions of an axisymmetric geometry and a flow that does not vary in axial direction.

In a numerical study performed within the EU project AMICAL, no added value was found of using in-duct Green's functions for beamforming. On the contrary, a simple delay-and-sum approach, neglecting wall reflections, seems to be the most robust.

While the numerical study was restricted to uniform flow, the current paper considers delay-and-sum beamforming in a non-uniform swirling flow typical for a fan-stator stage. The time delay between microphones and potential acoustic sources is calculated with the ray tracing technique[14]. The main challenge herein is finding the eigenrays that connect sources and microphones. A fast iteration method[15] is proposed for that.

To examine the merits of this beamforming approach, a numerical test set-up was defined that mimics as much as possible a real engine. This test case is described in Section II. The method to calculate time delays is summarized in Section III. Beamforming results follow in Section IV. Conclusions and future outlook are formulated in Section V.

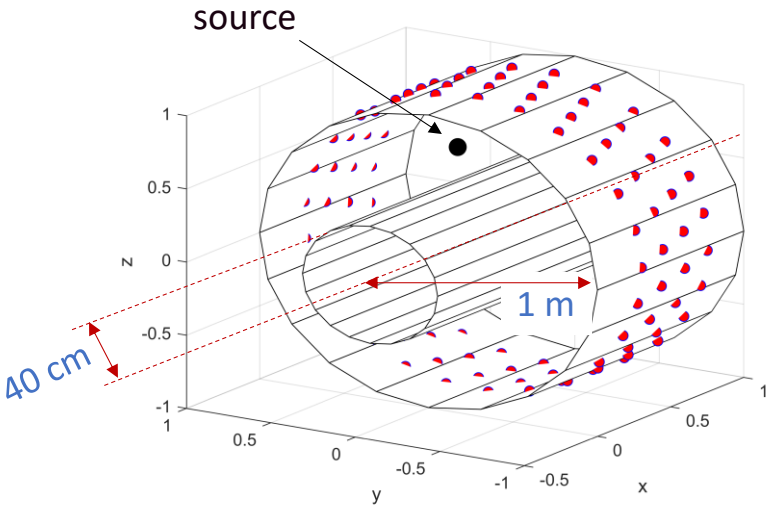

Figure 1 Sketch of test case geometry

II. Test case

For the test case, we loosely follow the high-speed flow case of Mathews and Peake[12]. The hub radius is $h = 0.4$ m and the tip radius is $R = 1$ m. Cartesian coordinates x, y, z are used; the x-axis coincides with the duct axis. The flow is in positive x-direction. A point source is located halfway hub and casing, at $\vec{\xi} = (0, 0, 0.7)$, see Figure 1. The microphone array is a "cage array" in the outer wall, consisting of 4 rings of 25 equally spaced microphones. The axial spacing between the microphone rings is 0.1 m. The first ring is located at $x = 0.1$.

The point source emits sound at the following dimensionless frequencies (Helmholtz numbers):

$$\mathrm{He} = 2\pi f R / c_0 = 10,\ 20,\ 30,\ 40, \tag{1}$$

where c_0 is the sound speed at the tip: $c_0 = 340$ m/s. Consequently, the considered frequencies are

$$f = 541,\ 1082,\ 1623,\ 2165\ \mathrm{Hz}. \tag{2}$$

By the method of Brouwer and Sijtsma[13] (using 61 radial segments) the microphone responses were calculated both with and without outer wall liner, of which the dimensionless impedance depends on He:

$$Z = 1 - i\cot(\mathrm{He}/40). \tag{3}$$

Note that this expression assumes the $\exp(+2\pi i f t)$ sign convention.

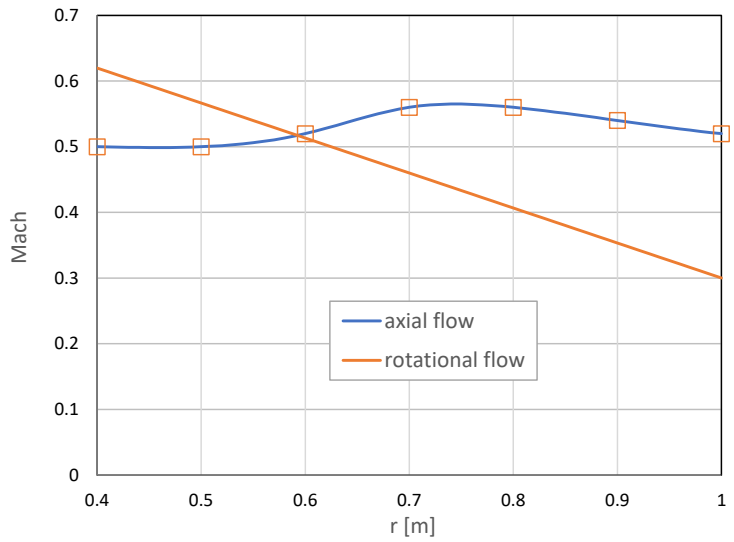

Figure 2 Mach numbers of axial and rotational flow

The swirling flow consists of an axial and a rotational component:

$$\vec{U}(\vec{x}) = \begin{pmatrix} U_x(\vec{x}) \\ U_y(\vec{x}) \\ U_z(\vec{x}) \end{pmatrix} = c_0 M_x(r) \begin{pmatrix} 1 \\ 0 \\ 0 \end{pmatrix} + c_0 M_\theta(r) \begin{pmatrix} 0 \\ z/r \\ -y/r \end{pmatrix}, \tag{4}$$

with $r = \sqrt{y^2 + z^2}$. The Mach numbers $M_x(r)$ and $M_\theta(r)$ are plotted in Figure 2. The axial Mach number is defined by interpolation through the points in the table below.

r	0.4	0.5	0.6	0.7	0.8	0.9	1.0
M_x	0.5	0.5	0.52	0.56	0.56	0.54	0.52

For the Mach number of the rotational flow, a linear relationship is used:

$$M_\theta(r) = \alpha r + \beta, \tag{5}$$

with

$$\begin{cases} \alpha = \left(M_{\theta,\mathrm{tip}} - M_{\theta,\mathrm{hub}}\right) / (R - h), \\ \beta = \left(M_{\theta,\mathrm{hub}} R - M_{\theta,\mathrm{tip}} h\right) / (R - h). \end{cases} \tag{6}$$

The Mach numbers at hub and tip are $M_{\theta,\mathrm{hub}} = 0.62$ and $M_{\theta,\mathrm{tip}} = 0.3$, respectively.

Inside the duct, we assume an r-dependent sound speed, following Eq. (8) of Mathews and Peake[12]:

$$c^2(r) = c_0^2 - (\gamma - 1)\int_r^R \frac{U_\theta^2(s)}{s} ds \,. \tag{7}$$

III. Time delay calculation

As stated in the Introduction, beamforming is done with a simple delay-and-sum algorithm. Let $\vec{\xi}$ be a potential source position, $\vec{x}_n$ the location of the *n*-th microphone, $p_n(t)$ the measured acoustic signal, Δt the time delay between source and microphone and *N* the number of microphones, then the source signal *a* is retrieved by:

$$a(\vec{\xi}, t) = \frac{1}{N}\sum_n p_n\left(t + \Delta t(\vec{\xi}, \vec{x}_n)\right). \tag{8}$$

Note that Eq. (8) does not include a correction for distance between source and microphones. Hence, the level of the source signal is "as measured by the array". The frequency-domain equivalent of Eq. (8) is

$$A(\vec{\xi}, f) = \frac{1}{N}\sum_n P_n(f)\exp\left(2\pi i f \Delta t(\vec{\xi}, \vec{x}_n)\right). \tag{9}$$

The calculation of the time delay between a source $\vec{\xi}$ and a microphone $\vec{x}_n$ is done with the technique of ray tracing[13]. Starting point is the following expression for the infinitesimal time delay:

$$c\,dt = \left\| d\vec{x} - \vec{U}dt \right\|. \tag{10}$$

The wave-slowness vector $\vec{k}$ is introduced as the gradient of *dt* with respect to $d\vec{x}$. By definition, this vector is perpendicular to the wave front. Implicit differentiation of Eq. (10) yields

$$\vec{k} = \frac{d\vec{x} - \vec{U}dt}{\vec{U}\cdot d\vec{x} + \left(c^2 - U^2\right)dt}. \tag{11}$$

From Eqs. (10) and (11), the eikonal equation can be derived (with $k = \left\|\vec{k}\right\|$):

$$c^2k^2 = \left(1 - \vec{k}\cdot\vec{U}\right)^2. \tag{12}$$

With Fermat's principle, the following differential equations follow for the ray $\vec{x}(t)$ and the corresponding wave-slowness vector $\vec{k}(t)$:

$$\begin{cases} \dfrac{d\vec{x}}{dt} = c\dfrac{\vec{k}}{k} + \vec{U}, \\ \dfrac{d\vec{k}}{dt} = -k\nabla c - \left(\vec{k}\cdot\nabla\right)\vec{U}. \end{cases} \tag{13}$$

Further evaluation of these ray tracing equations can be found in the appendix.

Acoustic rays $\vec{x}(t)$ are calculated by solving Eq. (13) with the classical 4-th order Runge-Kutta method, starting from a potential source location $\vec{x}(0) = \vec{\xi}$ and an initial "shoot" direction $d\vec{x}$. The corresponding initial wave-slowness vector $\vec{k}(0)$ is found with Eq. (11), after having solved *dt* from Eq. (10):

$$dt = \frac{-\vec{U}\cdot d\vec{x} + \sqrt{\left(\vec{U}\cdot d\vec{x}\right)^2 + \left(c^2 - U^2\right)dx^2}}{c^2 - U^2}. \tag{14}$$

The challenge is to find the shoot direction by which the acoustic ray "hits" the target microphone $\vec{x}_n$, i.e., the so-called eigenray. For that purpose, the following iteration procedure was implemented.

Consider ray tracing from a source $\vec{\xi}$ to a microphone $\vec{x}_n$. The "view direction" $\vec{v}_0$ is defined by

$$\vec{v}_0 = \frac{\vec{x}_n - \vec{\xi}}{\left\|\vec{x}_n - \vec{\xi}\right\|}. \tag{15}$$

Suppose $\vec{w}^{(j)}$ (with $\left\|\vec{w}^{(j)}\right\| = 1$) is the "shoot direction" at the *j*-th iteration step. The "end point" $\vec{x}^{(j)}$ on the ray can be defined as the point that minimizes the distance to the microphone $\vec{x}_n$. The view direction $\vec{v}^{(j)}$ towards the end point is defined by

$$\vec{v}^{(j)} = \frac{\vec{x}^{(j)} - \vec{\xi}}{\left\| \vec{x}^{(j)} - \vec{\xi} \right\|}. \tag{16}$$

For the updated shoot direction $\vec{w}^{(j+1)}$ we write

$$\vec{w}^{(j+1)} = \left(\vec{w}^{(j)} \cdot \vec{w}^{(j+1)} \right) \vec{w}^{(j)} + \left(\vec{w}^{(j)} \times \vec{w}^{(j+1)} \right) \times \vec{w}^{(j)}, \tag{17}$$

which is an identity that holds for any pair of 3D-vectors with unit norm.

The update $\vec{w}^{(j+1)}$ is found by rotating $\vec{w}^{(j)}$ by the same angle as the angle between $\vec{v}^{(j)}$ and $\vec{v}_0$ (see Figure 3). This is quantified by approximating the dot product and the cross product as follows:

$$\begin{cases} \vec{w}^{(j)} \cdot \vec{w}^{(j+1)} \approx \vec{v}^{(j)} \cdot \vec{v}_0, \\ \vec{w}^{(j)} \times \vec{w}^{(j+1)} \approx \vec{v}^{(j)} \times \vec{v}_0. \end{cases} \tag{18}$$

Thus, the updated shoot direction is

$$\vec{w}^{(j+1)} = \left(\vec{v}^{(j)} \cdot \vec{v}_0 \right) \vec{w}^{(j)} + \left(\vec{v}^{(j)} \times \vec{v}_0 \right) \times \vec{w}^{(j)}. \tag{19}$$

This iteration procedure leads to a rapid convergence.

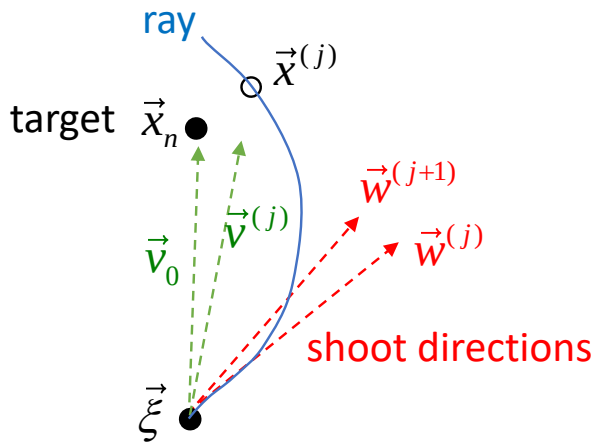

Figure 3 Illustration of ray tracing iterations

IV. Results

Beamforming is done from points on a cross-section scan plane that includes the actual source (see Figure 4). In a set-up like this, not every microphone can be reached from every scan point. This is illustrated in Figure 5. For many pairs of scan points and microphones, a direct acoustic ray does not exist, because of the presence of the hub and the rotational flow gradient. This is not a real problem. Beamforming can be done with the available microphones. In fact, this is beneficial, as the signals of the further-away microphones contain more reflections.

A remarkable feature in Figure 5 is the asymmetry. The microphones in the direction of the flow rotation can be reached more easily than the upstream microphones. To obtain more symmetry and to further reduce the effects of wall reflections, beamforming was limited to pairs of scan points and microphones at less than 0.7 m distance. The remaining acoustic rays are depicted in Figure 6.

Beamforming results with the hard duct wall are shown in Figure 7. The source is located at almost the correct position. Some side lobe levels are quite high. Beamforming results with the lined duct wall are shown in Figure 8. The side lobe levels are now significantly lower.

To highlight the importance of including rotational flow in the time delay calculations, beamforming was also done while ignoring the rotational flow component. Figure 9 shows the results with the lined duct. Comparison with Figure 8 shows that the source location shifts in the direction of the swirl. The peak levels are a few dB lower and the relative side lobe levels increase significantly.

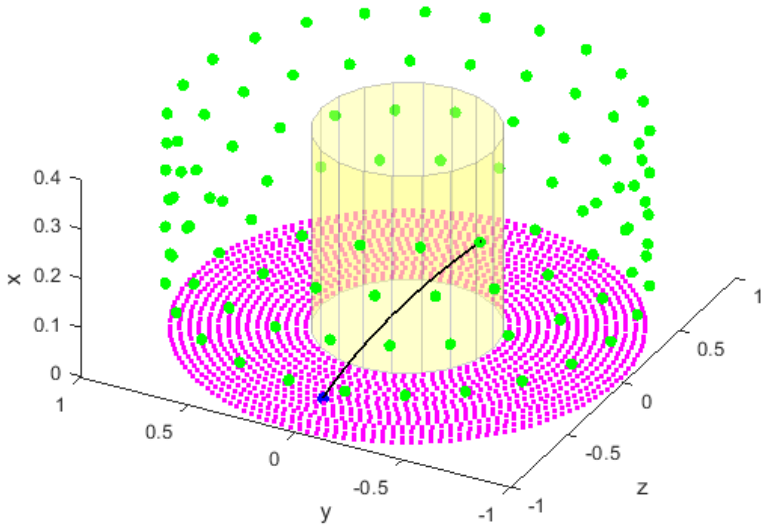

Figure 4 Array (green), scan plane (magenta) and typical acoustic ray

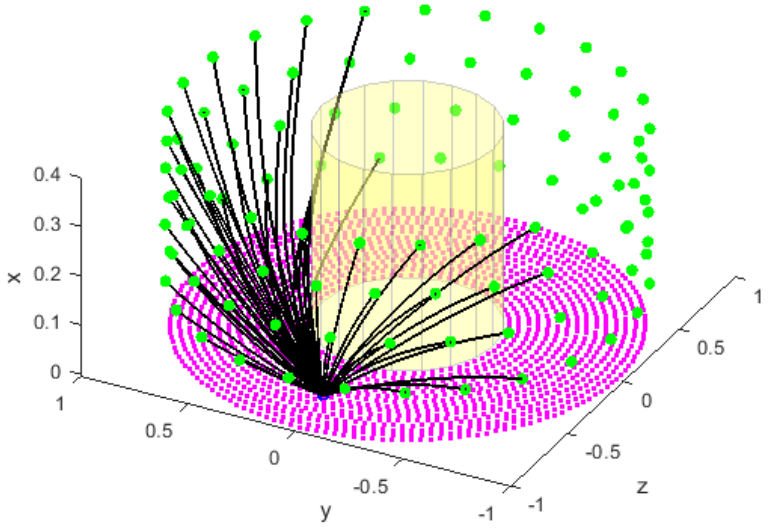

Figure 5 All direct acoustic rays from a scan point

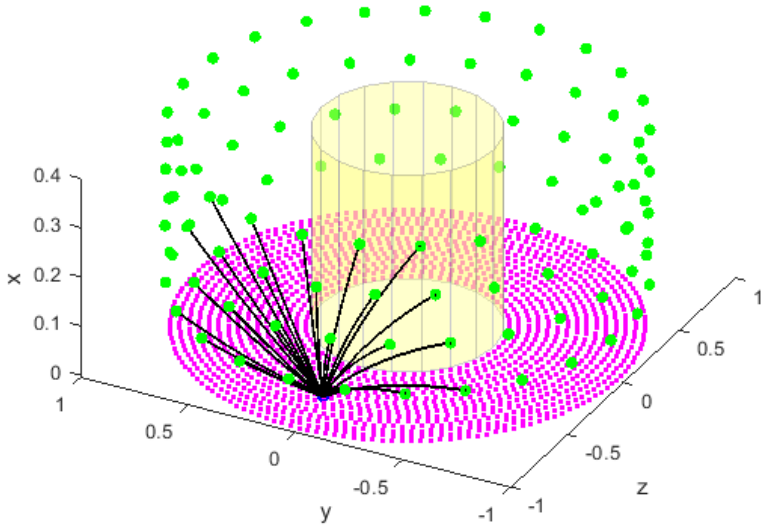

Figure 6 Rays selected for beamforming

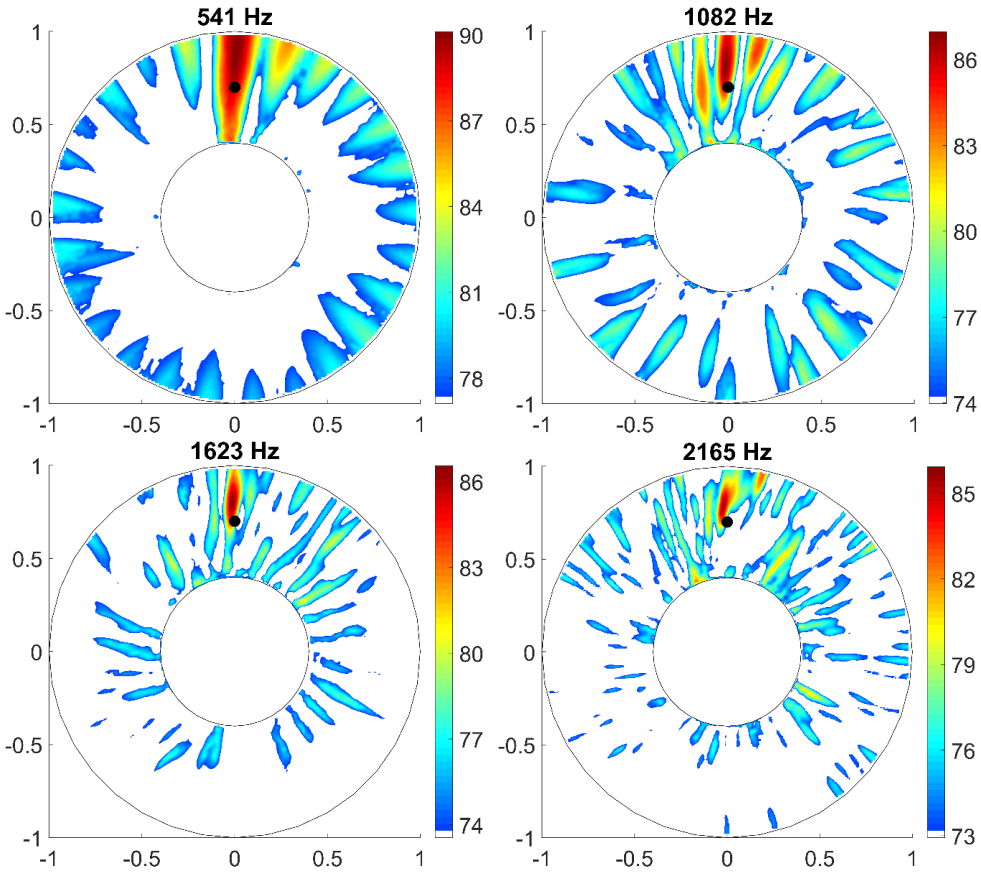

Figure 7 Beamforming results with hard duct wall

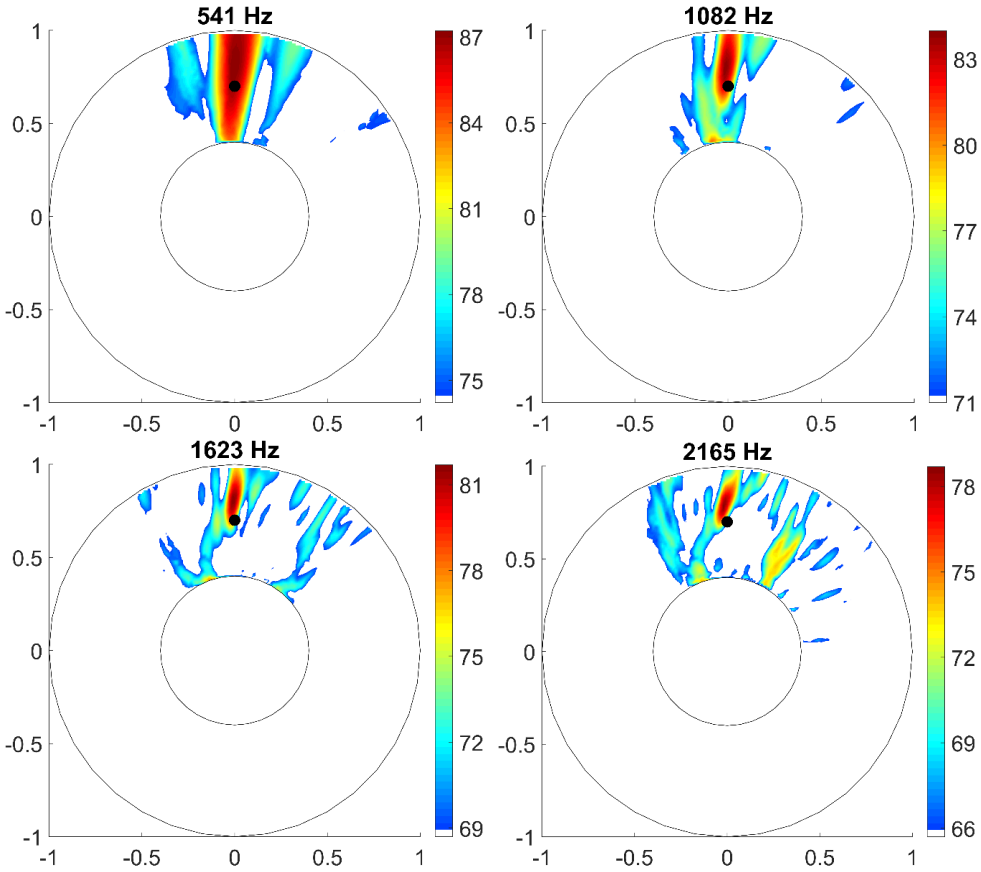

Figure 8 Beamforming results with lined duct wall

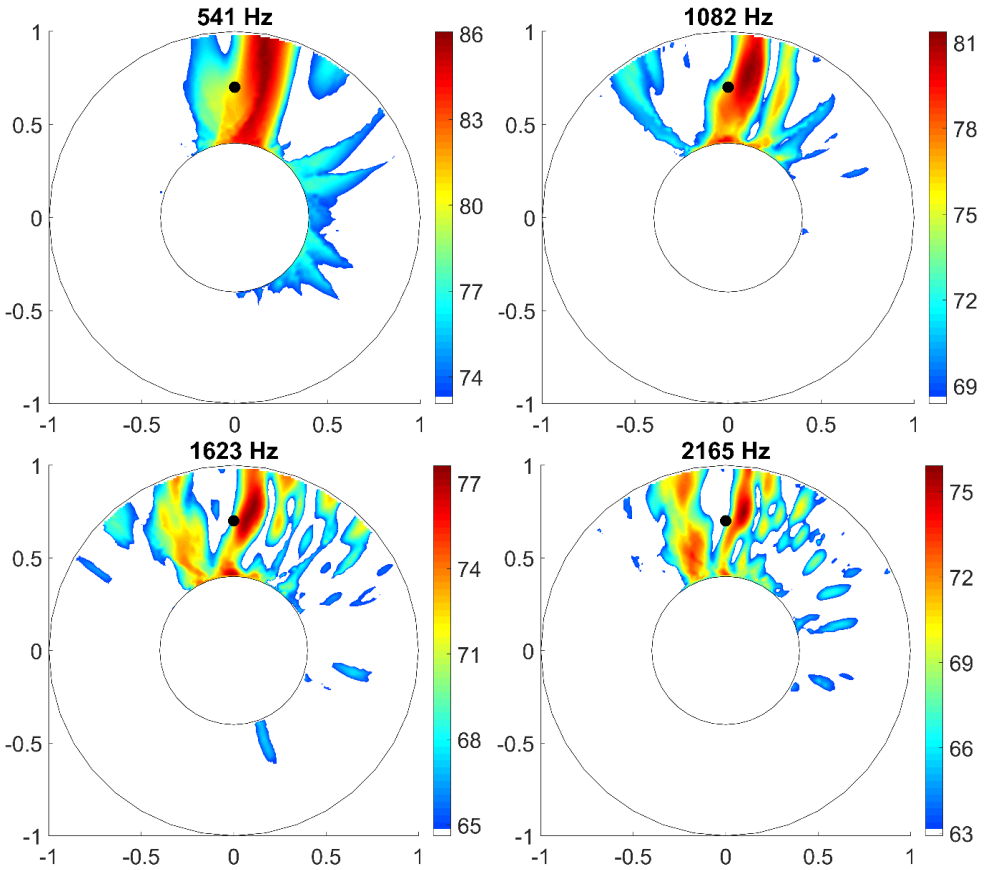

Figure 9 Beamforming results with lined duct wall; time delays calculated without swirl

V. Conclusions and future outlook

Beamforming in an annular duct with a realistic swirling flow is feasible. This was demonstrated by delay-and-sum beamforming in which the time delay from scan points to microphones was obtained by ray tracing. The eigenrays were found by a rapid iteration procedure. For each scan point a limited number of microphones was used, as not every microphone can be reached via a direct ray. To minimize the effect of wall reflections, the number of microphones per scan point was reduced further. The steering vectors did not contain corrections for distance. Including a wall liner leads to improved beamforming results.

In this paper, only beamforming at fixed frequencies was considered. The extension to the common practice (long time duration, averaging over snapshots to obtain a cross-spectral matrix) is straightforward. The only new feature is that steering vectors contain many zero elements. How this affects typical deconvolution methods like DAMAS[3] and CLEAN-SC[4] is a topic for further investigation.

Beamforming on a rotating scan grid can be done without too much additional computation time by obtaining time delays via interpolation[15]. This requires a sufficiently high scan point density. Reduction of computation time can be achieved by using eigenray shoot directions as initial shoot directions from neighboring scan points.

An important final remark is that the beamforming approach of this paper is not restricted to axisymmetric geometries. In fact, it can be applied to any geometry, as long as the flow speed and the sound speed are known in sufficient detail.

Acknowledgment

This major part of this work was performed within the AMICAL project, which has received funding from the Clean Sky 2 Joint Undertaking under the European Union's Horizon 2020 research and innovation programme under grant agreement no 886733. This publication reflects only the authors' view and the JU is not responsible for any use that may be made of the information it contains.

References

[1]Sijtsma, P., "Acoustic Beamforming for the Ranking of Aircraft Noise", Published in *Accurate and Efficient Aeroacoustic Prediction Approaches for Airframe Noise*, VKI Lecture Series 2013-03, Edited by C. Schram, R. Dénos, and E. Lecomte, March 25-29, 2013.

[2]Moreau, S., "Turbomachinery Noise Predictions: Present and Future", *Acoustics*, Vol. 1 (1) , 2019, pp. 92-116.

[3]Brooks, T.F., and Humphreys, W.M., "A Deconvolution Approach for the Mapping of Acoustic Sources (DAMAS) Determined from Phased Microphone Arrays", *Journal of Sound and Vibration*, Vol. 294, 2006, pp. 856-879.

[4]Sijtsma, P., "CLEAN Based on Spatial Source Coherence", *International Journal of Aeroacoustics*, Vol. 6, No. 4, 2007, pp. 357-374.

[5]Merino-Martínez, R., Sijtsma, P., Rubio Carpio, A., Zamponi, R., Luesutthiviboon, S., Malgoezar, A.M.N., Snellen, M., Schram, C., and Simons, D.G., "Integration Methods for Distributed Sound Sources", *International Journal of Aeroacoustics*, Vol. 18 (4-5), 2019, pp. 444-469.

[6]Sijtsma, P., "Using Phased Array Beamforming to Identify Broadband Noise Sources in a Turbofan Engine", *International Journal of Aeroacoustics*, Vol. 9 (3), 2010, pp. 357-374.

[7]Lowis, C.R. and Joseph, P., "A Focused Beamformer Technique for Separating Rotor and Stator-Based Broadband Sources", AIAA Paper 2006-2710.

[8]Sijtsma, P., "Circular Harmonics Beamforming with Multiple Rings of Microphones", AIAA Paper 2012-2224, 2012.

[9]Dougherty, R.P., and Walker, B.E., "Virtual Rotating Microphone Imaging of Broadband Fan Noise", AIAA Paper 2009-3121.

[10]Rienstra, S.W., and Tester, B.J., "An Analytic Green's Function for a Lined Circular Duct Containing Uniform Mean Flow," AIAA Paper 2005-3020, May 2005.

[11]Sijtsma, P., "Green's Functions for In-Duct Beamforming Applications", AIAA Paper 2012-2248.

[12]Mathews, J.R. and Peake, N., "The Acoustic Green's Function for Swirling Flow in a Lined Duct", *Journal of Sound and Vibration*, Vol. 395, p. 294, 2017.

[13]Brouwer, H.H., and Sijtsma, P., "Phased Array Beamforming to Identify Broadband Noise Sources in the Interstage Section of a Turbofan Engine", AIAA Paper 2019-2669.

[14]Pierce, A.D., *Acoustics: An Introduction to Its Physical Principles and Applications*, McGraw-Hill, 1981.

[15]Sijtsma, P., "Fast Calculation of Microphone Array Steering Vectors with Shear Flow", BeBeC-2018-S03.

Appendix: Elaboration of ray tracing equations

Insertion of $\vec{U} = c_0\vec{M}$ in Eq. (13) yields

$$\frac{d\vec{x}}{dt} = c\frac{\vec{k}}{k} + c_0\vec{M}, \quad \frac{d\vec{k}}{dt} = -k\nabla c - c_0\left(\vec{k}\cdot\nabla\right)\vec{M} . \tag{20}$$

Herein:

$$\left(\vec{k}\cdot\nabla\right)\vec{M} = \frac{-1}{r}\left\{\left(k_y y + k_z z\right)\left\{\frac{M_\theta(r)/r - M'_\theta(r)}{r}\begin{pmatrix}0\\ z\\ -y\end{pmatrix} - \begin{pmatrix}M'_x(r)\\ 0\\ 0\end{pmatrix}\right\} - M_\theta(r)\begin{pmatrix}0\\ k_z\\ -k_y\end{pmatrix}\right\}. \tag{21}$$

and

$$\nabla c = \frac{1}{r}\begin{pmatrix}0\\ y\\ z\end{pmatrix}c'(r). \tag{22}$$

For the derivative of M_θ we have

$$M'_\theta(r) = \alpha . \tag{23}$$

The derivative of *c* is calculated from Eq. (7):

$$2c(r)c'(r) = \frac{d}{dr}c^2(r) = (\gamma-1)\frac{U_\theta^2(r)}{r}, \tag{24}$$

which implies

$$c'(r) = \frac{1}{2}(\gamma-1)\frac{c_0^2}{c(r)}\frac{M_\theta^2(r)}{r} . \tag{25}$$

The sound speed is evaluated as

$$c(r) = c_0\sqrt{1-(\gamma-1)\left[\frac{1}{2}\alpha^2\left(R^2-r^2\right) + 2\alpha\beta(R-r) - \beta^2\ln\left(\frac{r}{R}\right)\right]} . \tag{26}$$